THE JOURNAL OF BIOLOGICAL CHEMISTRY
Vol. 276, No. 17, Issue of April 27, pp. 14059–14066, 2001

Printed in U.S.A.

The 8-kDa Dynein Light Chain Binds to Its Targets via a Conserved (K/R)*X*TQT Motif*

Received for publication, November 14, 2000, and in revised form, January 8, 2001
Published, JBC Papers in Press, January 8, 2001, DOI 10.1074/jbc.M010320200

Kevin W.-H. Lo‡, Scott Naisbitt§, Jing-Song Fan‡, Morgan Sheng§¶, and Mingjie Zhang‡‖

From the ‡Department of Biochemistry, The Hong Kong University of Science and Technology, Clear Water Bay, Kowloon, Hong Kong, People's Republic of China and the §Howard Hughes Medical Institute and Department of Neurobiology, Massachusetts General Hospital and Harvard Medical School, Boston, Massachusetts 02114

Cytoplasmic dynein is a large, multisubunit molecular motor that translocates cargoes toward the minus ends of microtubules. Proper functioning of the dynein motor requires precise assembly of its various subunits. Using purified recombinant proteins, we show that the highly conserved 8-kDa light chain (DLC8) binds to the intermediate chain of the dynein complex. The DLC8-binding region was mapped to a highly conserved 10-residue fragment (amino acid sequence SYSKETQTPL) C-terminal to the second alternative splicing site of dynein intermediate chain. Yeast two-hybrid screening using DLC8 as bait identified numerous additional DLC8-binding proteins. Biochemical and mutational analysis of selected DLC8-binding proteins revealed that DLC8 binds to a consensus sequence containing a (K/R)*X*TQT motif. The (K/R)*X*TQT motif interacts with the common target-accepting grooves of DLC8 dimer. The role of each conserved amino acid residue in this pentapeptide motif in supporting complex formation with DLC8 was systematically studied using site-directed mutagenesis.

Cytoplasmic dynein is a microtubule-based molecular motor that has been implicated in a wide variety of functions including retrograde organelle movement, nuclear migration, mitotic spindle alignment, and axonal transport (1–3). The enzyme is a multisubunit complex assembly containing two molecules of heavy chains (DHC[1], ~530 kDa), several intermediate chains (DIC, ~74 kDa) and light intermediate chains (DLIC, 53–59 kDa), and a number of light chains (DLC, 8–22 kDa). The heavy chains of dynein contain ATPase activity essential for force generation and are also responsible for attaching the motor complex to microtubules. The divergent N-terminal one-third of DHC contains the DIC-binding site. DICs may function as linkers of cargoes to the dynein motor through direct binding to dynactin (4). The functions of other dynein polypeptides are largely unknown.

The 8-kDa light chain (DLC8) of cytoplasmic dynein was originally identified as a light chain of *Chlamydomonas* outer arm axonemal dynein (5–7). The protein was subsequently shown to be a stoichiometric component of cytoplasmic dynein and of actin-based motor myosin V (8). Mutational studies showed that DLC8 is required for proper functioning of cytoplasmic dynein including retrograde intraflagellar transport (9), nuclear migration, and motor complex localization (10). However, it is not known how DLC8 is assembled into the cytoplasmic dynein motor complex, although it was suggested that the protein is associated with DIC in the axonemal dynein complex (6).

DLC8 contains 89 amino acid residues and is highly conserved throughout evolution (>90% amino acid sequence identity from *Caenorhabditis elegans* to humans). Other than binding to certain subunits of motor proteins, DLC8 has also been shown to interact with several cellular targets with diverse functions. DLC8 binds to neuronal nitric-oxide synthase (11, 12), proapoptotic Bcl-2 family protein Bim (13), *Drosophilia* mRNA localization protein Swallow (14), transcriptional regulator IκB (15), and postsynaptic scaffold protein GKAP (16). The DLC8-binding domain of nNOS was mapped to a short stretch of amino acid residues (12, 17). The other known DLC8-binding proteins neither contain homologous DLC8-interacting sequences found in nNOS nor bear obvious amino acid sequence similarities among each other. Elucidation of the molecular basis of the interactions between DLC8 and its diverse target proteins represents an important step in understanding the function of this versatile protein. Structural studies showed that DLC8 contains two identical target-binding grooves located at opposite faces of the protein dimer interface (18). DLC8 is capable of binding to short peptide fragments of ~10 amino acid residues from its targets. The target peptides bind to DLC8 in an antiparallel β-strand structure by pairing with the β-strand located at the base of each target-accepting groove (17, 18).

We report here that DLC8 binds to a conserved (K/R)*X*TQT amino acid sequence motif in a wide variety of protein partners. Such a motif is present in DIC of cytoplasmic dynein and mediates association of DLC8 and DIC in the dynein complex.

MATERIALS AND METHODS

Yeast Two-hybrid Screen of DLC8-binding Proteins—Yeast-two hybrid screening was performed as described previously (16). Briefly, DLC8 was subcloned into pBHA (LexA fusion vector) and used to separately screen ~1 × 10^6 clones each from human and rat cDNA libraries constructed in pGAD10 (GAL4 activation vector; CLONTECH).

Expression Constructs—The full-length mouse DIC gene was constructed by assembling three partially overlapping genomic clones using standard PCR and DNA ligation methods. The DIC fragments were generous gifts from Dr. L. C. Tsui (20). The full-length DIC coding DNA fragment was inserted into the *Eco*RI/*Bam*HI sites of an in-house-

* This work was partially supported by Grants HKUST6084/98M, 6198/99M, and 6207/00M from the Research Grant Council of Hong Kong to M. Z.) and by the Human Frontier Science Program. The costs of publication of this article were defrayed in part by the payment of page charges. This article must therefore be hereby marked "*advertisement*" in accordance with 18 U.S.C. Section 1734 solely to indicate this fact.

¶ Assistant Investigator of the Howard Hughes Medical Institute.
‖ To whom correspondence should be addressed. Tel.: 852-2358-8709; Fax: 852-2358-1552; E-mail: mzhang@ust.hk.

[1] The abbreviations used are: DHC, dynein heavy chain; DIC, dynein intermediate chain; DLIC, dynein light intermediate chain; DLC, dynein light chain; PCR, polymerase chain reactions; GST, glutathione *S*-transferase; SDS-PAGE, SDS-polyacrylamide gel electrophoresis; nNOS, neuronal nitric-oxide synthase; HSQC, heteronuclear single quantum correlation.

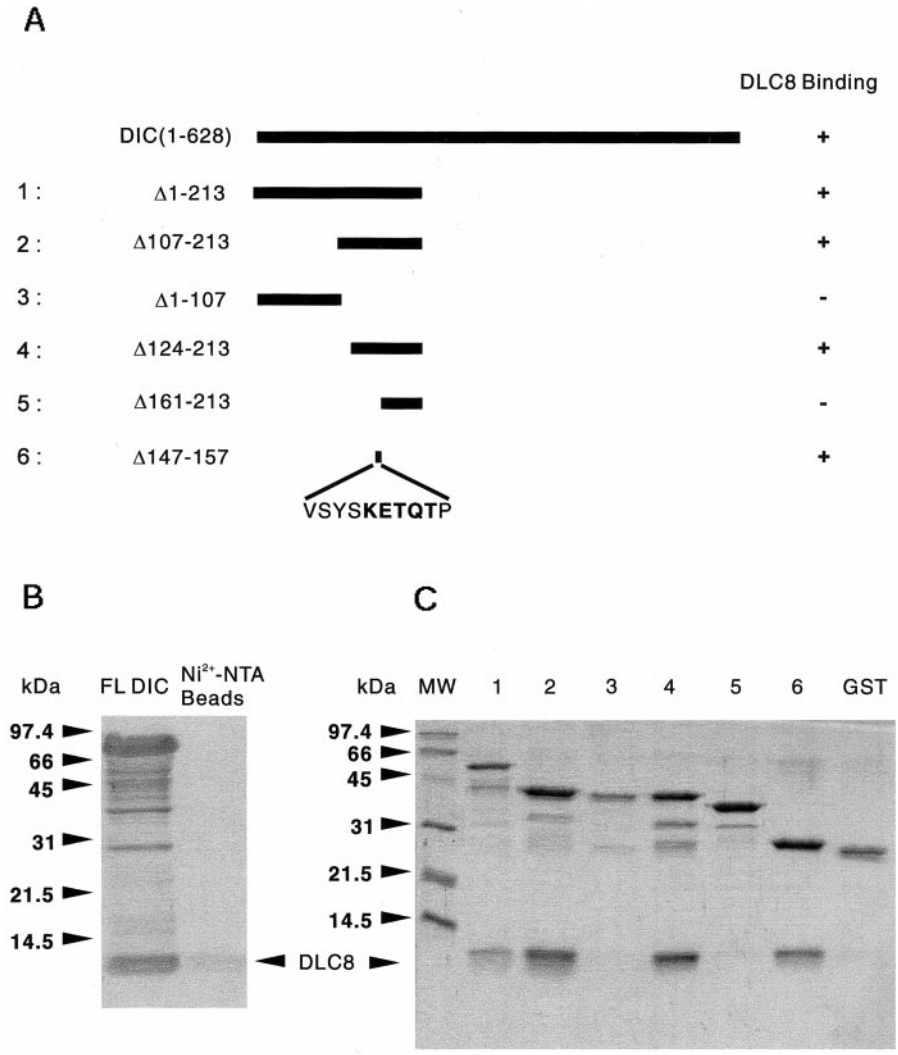

FIG. 1. **Mapping of the DLC8-binding site in DIC.** *A*, schematic diagram of full-length DIC and various DIC fragments used for assaying binding to DLC8. To facilitate refolding, the full-length DIC was expressed as a His-tagged protein. All of the DIC fragments were fused to GST. The binding of various forms of DIC with DLC8 is also summarized in the figure. *B* and *C*, Coomassie Blue staining of SDS-PAGE gels showing the interactions between various purified DIC fragments and DLC8. For the full-length (*FL*) DIC, Ni^{2+}-nitrilotriacetic acid (*Ni^{2+}-NTA*) beads were used as a negative control in the binding experiment (*B*). The Ni^{2+}-nitrilotriacetic acid beads contain some nonspecific binding to DLC8. To avoid possible confusion, the rest of the DIC fragments were prepared as GST fusion proteins. Purified GST was used as the negative control for the binding interactions between DIC fragments and DLC8. The lane numbers in *C* correspond to the construct numbers in *A*. *MW*, molecular weight markers.

modified pET32a plasmid vector (Novagen). Various truncation and point mutants of DICs were cloned into pGEX-4T-1 vector (Amersham Pharmacia Biotech) using standard recombinant DNA methods. The plasmids harboring the full-length DIC gene and various mutant DIC genes were transformed into *Escherichia coli* BL21(DE3) host cells for fusion protein production.

The C-terminal fragment of c82 (gene product of clone 82 identified from a yeast two-hybrid screening for DLC8-binding proteins; see Table I) containing amino acid residues 119–199 of the native protein was amplified by PCR using the coding strand primer 5′-CCGGAATTC-GAGAGATTGCAGGGTCTG-3′ and noncoding strand primer 5′-CCGCTCGAGCTAGAGGCTGGGTCTAC-3′. The PCR-amplified c82 fragment was inserted into the *Eco*RI/*Xho*I sites of pGEX-4T-1. Various GST-fused c82 truncation mutants used in this study were generated using standard PCR techniques. The GST-fused BS69 fragment was prepared using a method similar to that described for c82, except that two primers specific for BS69 were used in the PCR amplification.

Bacterial expression vectors of GST-fused Bim_L (long form) and Bim_S (short form), both lacking the hydrophobic transmembrane region and the BH3 domain, were constructed by PCR using full-length Bim_L and Bim_S (gifts from Dr. A. Strasser) as templates, respectively, using a pair of primers: 5′-CGGGGATCCATGGCCAAGCAAC-3′ (sense), and 5′-CCGCTCGAGTCACTCCTGTGCGATCC-3′ (antisense).

Expression and Purification of the Fusion Proteins—To express the full-length DIC and its truncated mutants, host cells transformed with the DIC expression plasmids were grown in LB medium at 37 °C until A_{600} reached ~1.2. The expression of the proteins was induced by the addition of isopropyl-1-thio-β-D-galactopyranoside to a final concentration of ~0.5 mM. Protein expression continued for ~3 h at 37 °C, and the cells were then harvested by centrifugation and stored at −80 °C prior to protein purification. The full-length DIC containing a hexahistidine tag at the N terminus was expressed in inclusion bodies. The pelleted bacterial cells were resuspended in 50 mM Tris-HCl buffer (pH 7.5) containing 2 mM EDTA, 1 mM phenylmethylsulfonyl fluoride, 1 μg/ml leupeptin, and 1 μg/ml antipain prior to cell lysis using sonication. The inclusion bodies were then washed extensively using 50 mM Tris-HCl buffer (pH 7.5) containing 1 M urea and 0.5% Triton X-100. The washed inclusion bodies were solubilized in 50 mM Tris-HCl buffer (pH 7.9) containing 5 mM imidazole, 0.5 M NaCl, and 6 M guanidine HCl at room temperature. The denatured protein was then passed through a Ni^{2+}-nitrilotriacetic acid affinity column following the procedure described by the manufacturer (Novagen) for proteins under denaturing conditions. Refolding of full-length DIC was achieved by a single step dialysis of the denatured protein against 1× phosphate-buffered saline buffer (pH 7.4). The refolded protein was recovered from the supernatant after centrifugation.

Various GST-fused DIC (as well as c82 and BS69) truncated and point mutants were expressed in soluble forms and purified using GSH-Sepharose affinity columns (Amersham Pharmacia Biotech) following the instructions of the manufacturer. The purified GST fusion proteins were dialyzed against 1× phosphate-buffered saline buffer (pH 7.4) to remove GSH, and the protein samples were directly used for DLC8 binding assay experiments. To express GST·Bim_L and GST·Bim_S, host cells containing the Bim plasmid constructs were grown in LB medium at 37 °C, reaching an A_{600} of ~1.0. The temperature of the bacterial cultures was then lowered to 25 °C before induction of GST·Bim expression. Purification of GST·Bim proteins followed the procedure described for the purification of the GST·DIC mutant proteins. Preparation of pure and untagged DLC8 was described in our earlier work (12).

Pull-down and Peptide Competition Experiments—Direct interactions between DLC8 and various GST-fused proteins were assayed in phosphate-buffered saline buffer (pH 7.4). Equal molar amounts of DLC8 and one of the GST fusion proteins (0.6 nmol each) were mixed in 100 μl of the assay buffer. The GST fusion protein-DLC8 complexes were pelleted by 30 μl of fresh GSH-Sepharose beads. The pellets were

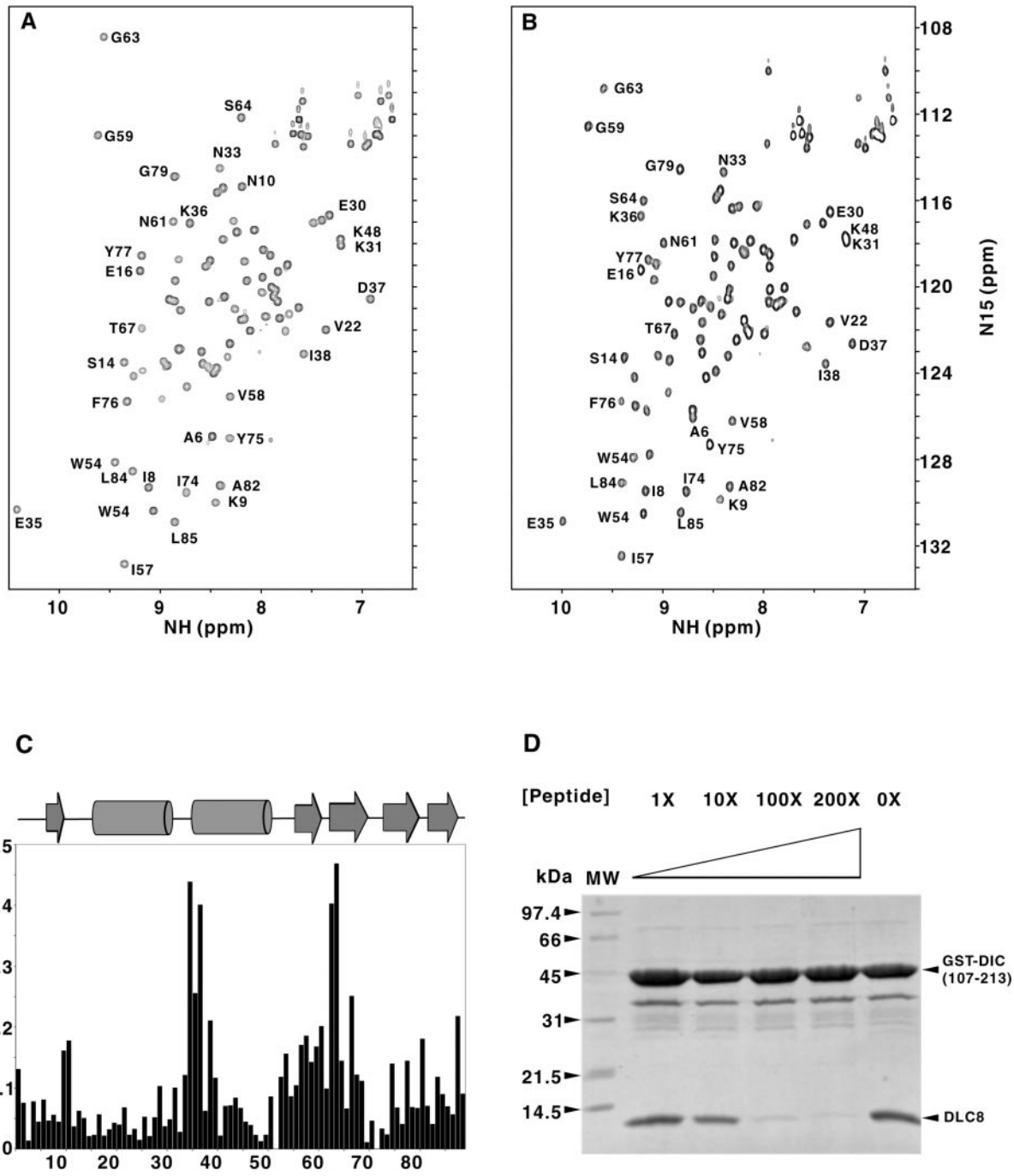

FIG. 2. **The DIC peptide specifically binds to DLC8.** ^{1}H,^{15}N HSQC spectra of ^{15}N-labeled free DLC8 (*A*) and the protein complexed with the DIC peptide (*B*). The assignments of selected amino acid residues of both free DLC8 and its complex with the DIC peptides are labeled with amino acid residue numbers and names. The large chemical shift changes of DLC8 resulting from DIC peptide binding indicate that DLC8 undergoes a significant conformational change upon binding to the DIC peptide. *C*, chemical shift changes of DLC8 resulting from the binding of the DIC peptide expressed using the minimal shift perturbation approach (19). The combined ^{1}H and ^{15}N chemical shift changes are defined according to Equation 1.

$$\Delta_{ppm} = \sqrt{(\Delta\delta_{HN})^2 + (\Delta\delta_N \cdot \alpha_N)^2} \quad \text{(Eq. 1)}$$

The scaling factor (α_N) used to normalize the ^{1}H and ^{15}N chemical shifts is 0.17. The secondary structure of DLC8 is also included in the figure. *D*, the DIC peptide competes with DIC for DLC8 in a dose-dependent manner. In this experiment, equimolar amounts of GST·DIC and DLC8 were mixed with increasing amounts of the DIC peptide. The remaining DLC8 complexed with GST·DIC was pulled down by GSH-Sepharose affinity beads and analyzed by SDS-PAGE followed by Coomassie Blue staining. *MW*, molecular weight markers.

washed three times with 0.5 ml of the assay buffer and subsequently boiled with 30 μl of 2× SDS-PAGE sample buffer. The intensity of the DLC8 band on SDS-PAGE gels was used to judge the strength of the interaction between DLC8 and various GST fusion proteins.

An 11-residue synthetic peptide (VSYSKETQTPL), corresponding to amino acid residues 147–157 of DIC, was commercially synthesized. To assay competition between the synthetic peptide and DIC for DLC8, increasing amounts of the peptide (from 0 to 200 molar ratio amounts of DIC) were included in the GST·DIC/DLC8 mixture. Residual GST·DIC-bound DLC8 was assayed using GSH-Sepharose affinity "pull-down" followed by SDS-PAGE as described above.

NMR Experiments—^{1}H,^{15}N HSQC spectra of ^{15}N-labeled DLC8 complexed with various synthetic peptides were acquired on a Varian Inova 500 MHz spectrometer equipped with a *z*-gradient shielded triple res-

TABLE I
DLC8-binding proteins identified through yeast two-hybrid screening

Protein name	Species	Binding mode	Remark
Myosin V	Human	Unknown	Transport via actin track
GKAP	Human, rat	Unknown	Protein transport
BS69	Rat	(K/R)*X*TQT	Adenovirus E1A-binding protein
c82	Human	(K/R)*X*TQT	Novel protein
AIBC1	Human, rat	Unknown	Potential oncogene
KIAA0710	Human	Unknown	Unknown function
c40	Rat	Unknown	Novel protein
c81	Human	Unknown	Novel protein

onance probe. All NMR spectra were recorded at 30 °C, with a protein concentration of ~0.5 mM dissolved in 100 mM potassium phosphate buffer, pH 7.0.

RESULTS

DLC8 Binds to an 11-Residue Fragment Located within a Highly Conserved Region of the N-terminal Domain of DIC—To understand how DLC8 is assembled in cytoplasmic dynein, we set out to identify the binding partner of DLC8 within the dynein complex. Given the overall similarity between axonemal and cytoplasmic dynein complexes, we suspected that DLC8 may also bind to DIC in cytoplasmic dynein. The gene encoding full-length DIC was assembled from three overlapping genomic clones (corresponding to the long form of DIC, GenBank™ accession number AF063229). His-tagged full-length DIC was expressed in *E. coli* cells and purified in its denatured form. DIC was successfully refolded, and the refolded DIC was assayed for its binding to DLC8. Affinity pull-down assay indicates that the full-length DIC binds directly to DLC8 (Fig. 1*B*). The circular dichroism spectrum of the refolded, full-length DIC indicated that the protein has a well folded structure in solution (data not shown).

To further define the DLC8-binding region, we created a series of truncation mutants of DIC as GST fusion proteins (Fig. 1*A*). The purified proteins were subsequently assayed for binding to DLC8 by simple mixing and GSH-Sepharose bead pull-down. The DLC8-binding region was mapped within the N-terminal domain of DIC (Fig. 1*C*). An 11-residue fragment corresponding to amino acid residues 147–157 (VSYS-**KETQT**PL) of DIC was sufficient to bind to DLC8 (Fig. 1*C*, *lane 6*).

We verified the interaction between DLC8 and the 11-residue peptide fragment of DIC derived from the truncation mapping experiment using two different approaches. In the first experiment, we titrated ^{15}N-labeled DLC8 with a synthetic peptide corresponding to residues 147–157 of DIC (the DIC peptide). Fig. 2, *A* and *B* show the ^{1}H,^{15}N HSQC spectra of DLC8 before and after binding to the DIC peptide. The chemical shift changes of DLC8 resulting from the DIC peptide binding are summarized using the minimal shift perturbation approach (Fig. 2*C*). These data show that the DIC peptide specifically binds to DLC8 and that the peptide-binding region is located at the target-binding groove formed by the β2, β3 strands, the loop linking β2 and β3, and part of the α2 helix (see "Discussion" for details). The observation of slow chemical exchange between the apo-DLC8 and peptide-bound DLC8 during titration indicates that the DIC peptide binds to DLC8 with a high affinity (data not shown). NMR titration experiments also showed that the DIC peptide binds to DLC8 with a 1:1 stoichiometry. In the second approach, we performed a binding competition experiment using the DIC peptide. Increasing molar amounts of the DIC peptide specifically competed with DIC protein for binding to DLC8 (Fig. 2*D*). As a negative control, an 11-residue peptide containing a partial Tctex-1-binding domain of DIC (amino acid sequence LGRRLHKLGVS) was found not to compete with DIC for binding to DLC8 (data not shown and Ref. 28).

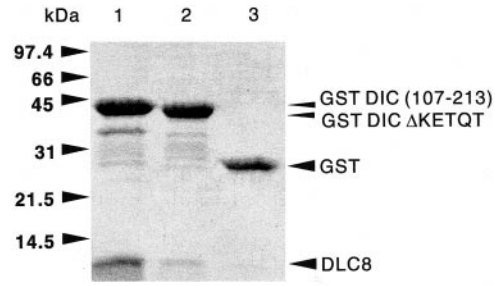

FIG. 3. **Deletion of the KETQT pentapeptide sequence from DIC disrupts its binding to DLC8.** Equivalent amounts of purified GST·DIC and GST·DIC(ΔKETQT) were used in the binding assay following the procedure described in the legend to Fig. 1*C*. Pure GST was used as a negative control in the experiment. The SDS-PAGE gel was stained with Coomassie Blue.

The 11-Residue Peptide Fragment Is the Only DLC8-binding Domain of DIC—The results presented in Figs. 1 and 2 demonstrate that the 11-residue peptide fragment (residues 147–157) of DIC is sufficient to bind to DLC8. Is this 11-residue fragment in DIC the only binding site for DLC8? To address this question, we disrupted the 11-residue DLC8-binding site by deleting residues 151–155 (KETQT) of DIC. This deletion mutant did not bind to DLC8, indicating that the 11-residue peptide fragment mapped in this study is the only DLC8-binding site in DIC (Fig. 3).

(K/R)XTQT Is a Common DLC8 Recognition Motif—To identify additional proteins that interact with DLC8, we performed a yeast two-hybrid screen using DLC8 as bait with both human and mouse brain cDNA libraries. A large number of specific interactors were isolated in the screen (see a partial list in Table I), many of which represent previously unidentified, potential DLC8-binding partners. We focus on a subset of the genes in Table I to study their interaction with DLC8.

The first gene we chose was clone 82 (c82), because the full-length sequence of c82 was recently deposited in GenBank™. The fragment isolated from the two-hybrid screen encodes the C-terminal half of the c82 protein (residues 119–199). The interaction between c82 and DLC8 was confirmed *in vitro* using purified recombinant proteins (Fig. 4). Using a series of deletion mutants, the DLC8-binding domain of c82 was mapped to a 14-residue peptide fragment with amino acid sequence ^{159}VGMHS**KGTQT**AKEE^{172} (Fig. 4).

The cDNA fragment of BS69 isolated from the DLC8 two-hybrid screen encodes amino acid residues 396–424 of the protein. GST-fused BS69-(396–424) robustly bound to DLC8 *in vitro*, indicating that the DLC8-binding region in BS69 is contained within this 29-amino acid segment (Fig. 5*A*). A stretch of amino acids similar to the DLC8-binding regions of DIC and c82 was noted within this 29-residue fragment, as was ^{410}MLH**RSTQT**TN^{419}.

The proapoptotic protein Bim was previously shown to interact specifically with DLC8, and the DLC8-binding domain was

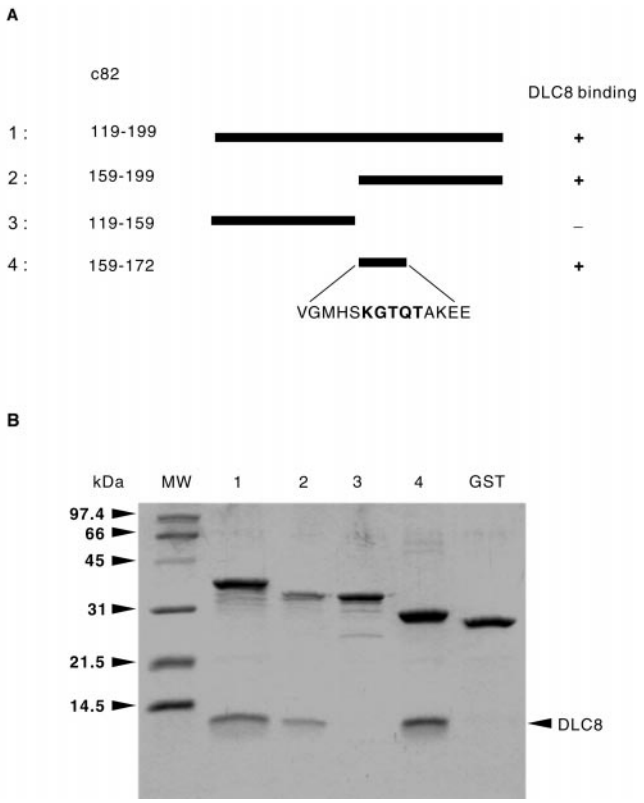

FIG. 4. **Mapping the DLC8-binding domain of c82.** *A*, schematic diagram showing the GST-c82 fragments used in the experiment. The amino acid sequence of the smallest DLC8-binding fragment is also shown in the figure. *B*, Coomassie Blue staining of the SDS-PAGE gel showing the interactions between various purified c82 fragments and DLC8. *MW*, molecular weight markers.

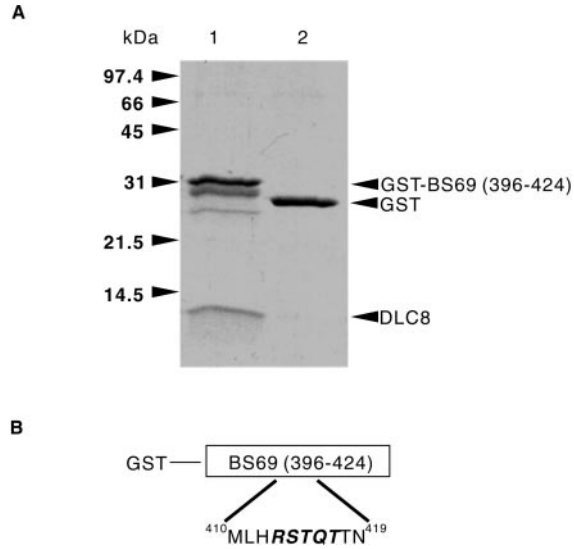

FIG. 5. **Interaction of the BS69 fragment with DLC8.** *A*, Coomassie Blue staining of the SDS-PAGE gel showing the interactions between DLC8 and a 29-residue fragment of BS69 fused with GST. This 29-residue fragment was identified six times in the yeast two-hybrid screening using DLC8 as bait. *B*, a partial amino acid sequence showing the potential DLC8-binding region of BS69.

mapped to a region of ~30 amino acid residues that were absent in the short form (Bim_S) of the alternatively spliced gene product (13). We confirmed this interaction between Bim_L and DLC8 *in vitro* using purified recombinant proteins (Fig. 6*A*). Additionally, we synthesized three overlapping peptides to map the minimal DLC8-binding domain of Bim_L (Fig. 6*B*). NMR titration of ^{15}N-labeled protein showed that all three peptides bound to the protein in an essentially identical manner (data not shown). The shortest peptide used in this experiment contains only nine amino acid residues (MSCD**KSTQT**). The $^{1}H,^{15}N$ HSQC spectrum of this 9-residue peptide-bound form of DLC8 is shown in Fig. 6*B*; the data suggest that this 9-residue peptide forms a stable complex with DLC8 (18).

We aligned the amino acid sequences of the DLC8-binding domains of various targets mapped in this study (Fig. 7). In this alignment, we also included putative DLC8-binding domains of Swallow and rabies virus P protein, two recently identified DLC8-binding proteins (14, 21, 22). The (K/R)*X*TQT motif was present in each of these DLC8 interactors and probably represents the consensus DLC8-binding sequence of these proteins (Fig. 7).

Mutational Analysis of the Consensus DLC8-binding Motif—To gain more insights into the interaction between DLC8 and the (K/R)*X*TQT motif, we mutated each consensus amino acid in the motif and assayed for the effect. To facilitate the binding assay, we fused the DLC8-binding domain of DIC with GST. In GST pull-down assays, mutation of the Gln residue in the (K/R)*X*TQT motif to either Ala or Gly completely abolished binding of the peptide to DLC8 (Fig. 8*B*). Mutation of either Thr residue in the motif to Gly also abolished interaction between the peptide and DLC8. Mutation of the first Thr (N-terminal to the Gln) to Ala greatly inhibited the binding, suggesting that the hydroxyl group of the Thr plays an active role in the complex formation. Mutation of the second Thr to Ser also significantly weakened the interaction, pointing to a possible role of the methyl group in the Thr side chain in peptide-DLC8 complex formation. Mutations of the Lys residue to a neutral Ala or a negatively charged Glu weakened the binding of the peptide to DLC8. However, the magnitude of the inhibition by the Lys mutations was lower than those observed with other point mutations. Taken together, the data in Fig. 8 indicate that all four consensus amino acid residues in the (K/R)*X*TQT motif play active roles in supporting productive complex formation between DLC8 and its target peptides. The data also indicate that the Thr-Gln-Thr tripeptide is likely to play a more dominant role in the peptide-DLC8 interaction.

DISCUSSION

As a multicomponent macromolecular complex, precise organization of various subunits of the dynein complex is essential for the motor to function properly. Recent molecular analysis of the cytoplasmic dynein complex has provided a detailed picture of the assembly of the DHC, DIC, and DLIC subunits in the motor complex (23, 24). However, little is known regarding the assembly of the light chains. Both cytoplasmic and axonemal dyneins share the highly conserved DLC8. In *Chlamydomonas* outer arm dynein, DLC8 was suggested to associate with the intermediate chains of the motor complex (7). By analogy, it was suggested that DLC8 is also assembled into the cytoplasmic dynein by binding to DIC subunits of the motor complex (8), although the flagellar and cytoplasmic DICs share limited sequence identity (particularly in the N-terminal half of the proteins). Using purified recombinant proteins, we show here that DLC8 can indeed bind to the full-length intermediate chain of cytoplasmic dynein (Fig. 1). An 11-residue fragment in the N-terminal half of DIC is necessary and sufficient for binding to DLC8. Our data is consistent with an earlier observation that DLC8 and DIC exist at a 1:1 stoichiometric ratio in cytoplasmic dynein (8).

Mammalian DIC is encoded by two different genes, and each gene generates multiple protein products by alternative splicing (4, 26). The 11-residue DLC8-binding domain of mouse DIC mapped in this study contains the amino acid sequence

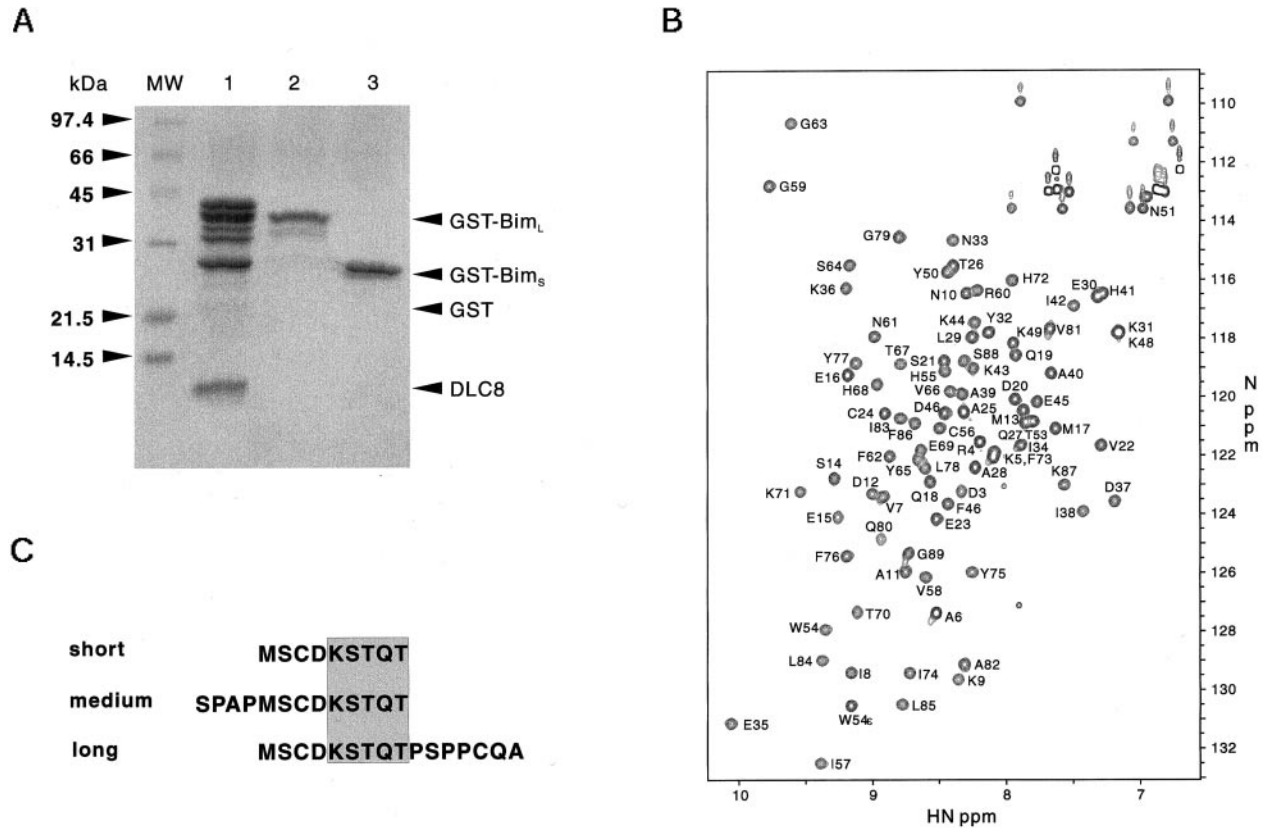

FIG. 6. **Interaction between Bim and DLC8.** *A*, Coomassie Blue staining of the SDS-PAGE gel showing the interaction between alternatively spliced forms of Bim (Bim$_L$ and Bim$_S$) with DLC8. *MW*, molecular weight makers. *B*, amino acid sequences of the three overlapping synthetic peptides used to map the minimal DLC8-binding domain of Bim. To study the interaction between the peptides and DLC8, we titrated ^{15}N-labeled DLC8 with each peptide to observe chemical shift changes of the ^{1}H,^{15}N HSQC spectra of the protein. *C*, ^{1}H,^{15}N HSQC spectrum of ^{15}N-labeled DLC8 complexed with the 9-residue Bim peptide shown in *B*. The assignment of the protein in the complex was obtained from our earlier work (18).

^{148}VSYSKETQTPL^{157}, and this fragment is located C-terminal to the second alternative splicing site of DIC. Within this 11-residue fragment, the 5-residue KETQT motif is likely to be responsible for the interaction of DIC to DLC8 (Figs. 6 and 8; see also Ref. 18). This 5-residue KETQT motif is present in all splice isoforms of both DIC gene products. Furthermore, the KETQT motif is highly conserved in cytoplasmic DICs throughout evolution (27). Given the fundamental roles that DLC8 plays in dynein motor function (9, 10), it might be expected that the DLC8-binding site should always remain available in various forms of DIC (and hence the dynein complex). We further note that the DLC8-binding domain does not overlap with the dynactin- and Tctex-1-binding sites of DIC, because dynactin binds to the first 120-amino acid residue fragment of DIC (4, 28). If DLC8 indeed acts as a dynein cargo adaptor, a single dynein complex may thus interact simultaneously with multiple cargoes.

The amino acid sequence of DLC8 is highly conserved throughout evolution, and the protein is ubiquitously expressed in various tissues. As such, DLC8 was proposed to be a multifunctional regulatory protein, in addition to functioning as a light chain of the dynein complex (11, 12, 25). To gain more insights into the range of proteins that interact with DLC8, we performed a yeast two-hybrid screen using DLC8 as bait. No obvious amino acid sequence homology or functional relationship can be identified among the proteins listed in Table I or among other proteins previously identified as binding to DLC8. Given that DLC8 can bind to short peptide fragments of ~10 amino acid residues (12, 17, 18), we performed detailed mapping analysis of DLC8-binding domains in several additional DLC8-binding proteins either identified from our yeast two-hybrid screen (c82 and BS69) or previously discovered (Bim).

DIC	^{146}VVSYS**KETQT**PLATH^{160}
Bim$_L$	^{47}PMSCD**KSTQT**PSPPC^{61}
c82	^{159}VGMHS**KGTQT**AKEEM^{173}
BS69	^{408}PRML H**RSTQT**TNDGV^{422}
Swallow	^{270}PASVP**KATQT**DHELL^{285}
P-PV	^{139}KSSED**KSTQT**TGREL^{153}

FIG. 7. **Sequence alignment of the DLC8-binding domains from its various targets.** The DLC8-binding domains mapped in this study are aligned with each other. The putative DLC8-binding domains of Swallow and rabies virus P protein (*P-PV*) are also included in this alignment. The consensus (K/R)*X*TQT motif in each sequence is highlighted with *bold letters*.

The DLC8-binding domains of these proteins are contained within short stretches of amino acids (9–29 amino acid residues). Sequence alignment analysis of the DLC8-binding domains immediately suggests that the 5-residue (K/R)*X*TQT sequence is a common DLC8 recognition motif in target proteins (Fig. 7). We also predict that DLC8 is likely to bind to Swallow via the ^{291}KATQT^{295} sequence immediately C-terminal to the coiled-coil domain of Swallow. Our prediction is consistent with experimental data showing that the DLC8-binding domain lies within amino acid residues 197–295 of Swallow (14). Recently, DLC8 was shown to interact with rabies virus P protein (the α subunit of RNA polymerase) via residues 138–172 of P protein (21, 22). Sequence alignments of P proteins from various strains of rabies virus showed that all contain a conserved KSTQT motif at the center of the protein. We suggest that DLC8 binds to P protein via this KSTQT motif. In the protein data base there are a large number of additional viral proteins containing a potential DLC8-binding (K/R)*X*TQT

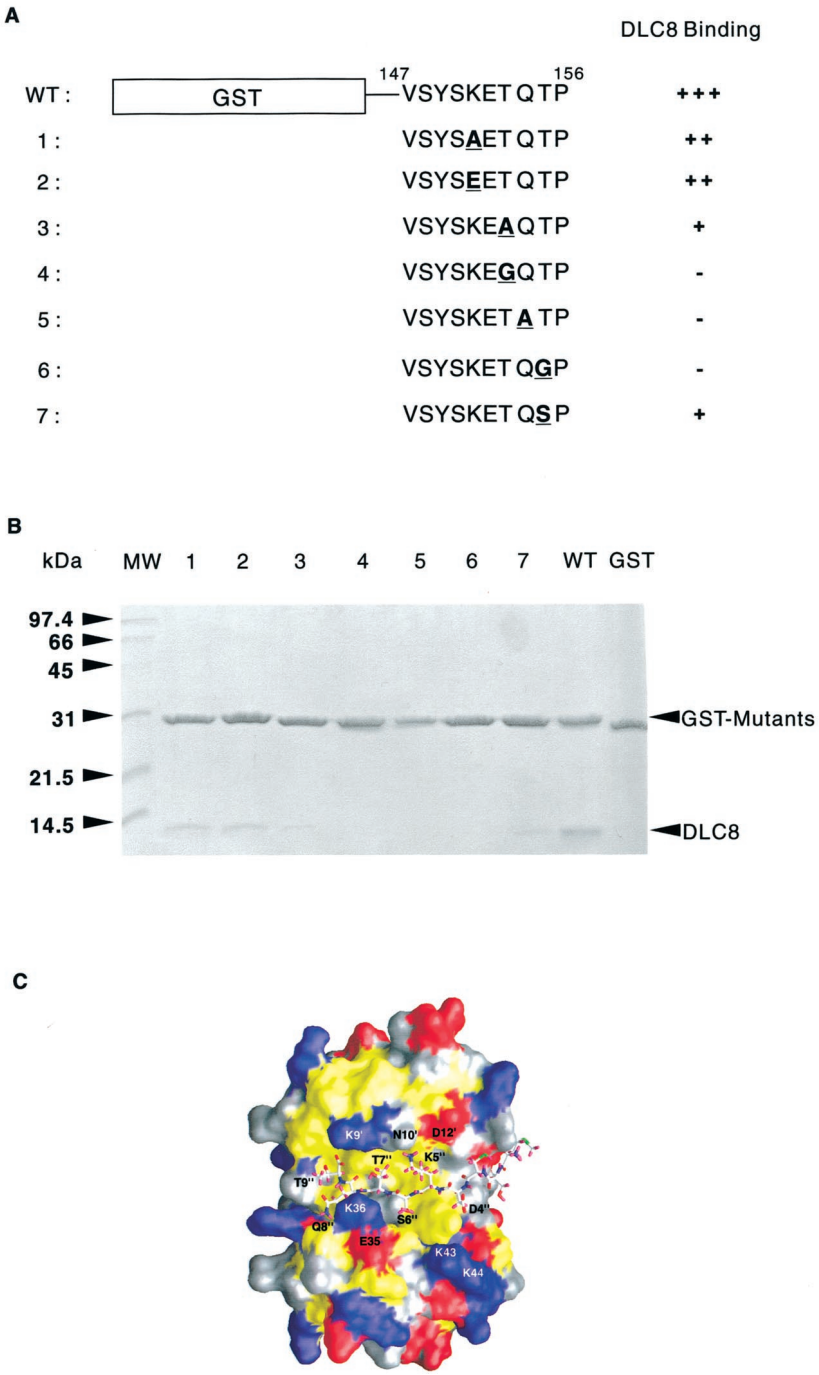

FIG. 8. **Mutational analysis of the roles of individual residues in the (K/R)*X*TQT motif in binding to DLC8.** *A*, schematic diagram showing the point mutations of the GST-fused DIC peptide used in the DLC8 binding assay. *WT*, wild type. *B*, Coomassie Blue staining of the SDS-PAGE gel showing the interactions between DLC8 and various GST·DIC peptide mutants. The wild type GST·DIC peptide and purified GST were used as positive and negative controls, respectively. The lane numbers in *B* match the construct numbers in *A*. *MW*, molecular weight markers. *C*, binding of a (K/R)*X*-TQT motif-containing peptide (the 9-residue DLC8-binding domain of Bim shown in Fig. 6) to DLC8. In this figure, the DLC8 dimer is shown in a surface model, and the peptide is in an explicit atom model. The positively charged amino acids in DLC8 are shown in *blue*; negatively charged residues are in *red*; hydrophobic residues are in *yellow*; and polar residues are in *gray*. The amino acid residues of DLC8 that form intimate electrostatic and hydrogen-bonding interactions are labeled with amino acid residue numbers and names (the numbers with and without a prime are used to differentiate residues from two different monomers of DLC8). The amino acid sequence of the peptide is labeled with residue name and number using double primes. The coordinates of the structure were taken from our earlier work (Ref. 18, Protein Data Bank code 1F95).

motif. For example, poly(A) polymerase catalytic subunit from vaccinia virus contains a ^{84}KQTQT^{88} motif. Human papillomavirus probable E4 protein contains a KQTQT motif in its N terminus. Several viral proteases (*e.g.* human adenovirus endoprotease and *Haemophilus influenzae* immunoglobulin A1 protease precursor) contain potential DLC8-binding KSTQT motifs. It is possible that DLC8 is responsible for dynein-mediated retrograde transport of these viral proteins along microtubules in infected cells (*e.g.* retrograde axonal transport of viral proteins in virus-infected neurons).

It is important to point out that the (K/R)*X*TQT motif is not the only DLC8 recognition sequence in target proteins. For example, the amino acid sequence of the DLC8-binding domain of nNOS is clearly different from the (K/R)*X*TQT motif (Fig. 7). We were not able to find a (K/R)*X*TQT motif in a number of other known DLC8-binding proteins including myosin V, GKAP, AIBC1, and KIAA0710. We showed earlier that DLC8 binds to a (K/R)*X*TQT motif-containing peptide and a peptide encompassing the DLC8-binding domain of nNOS with remarkably similar mechanisms, although the two peptides share little amino acid sequence identity (18). We have also shown that the structural and dynamic properties of the target-binding site of DLC8 is uniquely suited to bind to peptide fragments with diverse amino acid sequences without sacrificing target binding specificity and affinity.[2] Therefore, it is perhaps not surprising that DLC8 can bind a number of other target proteins, even though these proteins do not contain a (K/R)*X*TQT motif. We would also like to emphasize that the DLC8-binding proteins listed in Table I are only potential

[2] J.-S. Fan, Q. Zhang, H. Tochio, and M. Zhang, submitted for publication.

DLC8 targets, because we only used partial fragments of the proteins for binding studies. Further *in vitro* and *in vivo* studies are required to substantiate whether these proteins are genuine DLC8-binding targets under physiological conditions.

Our earlier structural studies showed that the (K/R)*X*TQT motif forms a β-strand structure in the DLC8-target peptide complex (Fig. 8*C*; see also Ref. 18). To establish a better structure-function relationship of the (K/R)*X*TQT motif-mediated DLC8 binding, the four conserved residues in the motif were systematically mutated. The structure of the DLC8 complexed with a (K/R)*X*TQT motif-containing peptide suggested that the binding affinity of the peptide to DLC8 is due to a combination of backbone hydrogen bonding and a number of hydrogen-bonding and electrostatic interactions between the side chains of the peptide and DLC8 (18). For example, strong hydrogen-bonding interactions between the side chain of the Gln residue in the peptide and side chains of Glu^{35} and Lys^{36} of DLC8 were observed. Mutation of the Gln to Ala, which eliminates the hydrogen-bonding capacity of the side chain of this amino acid residue, completely abolished peptide binding to DLC8 (Fig. 8). We believe that the Gln residue plays a central role in promoting the formation of the peptide-DLC8 complex. Structure-based sequence alignment of the nNOS peptide and the (K/R)*X*TQT motif peptide showed that a Gln residue in the nNOS peptide occupies the same position as the Gln residue in the (K/R)*X*TQT peptide upon formation of complexes with DLC8 (18). The total loss of the interaction observed in the individual Thr to Gly mutations is probably a combination of the loss of side chain interactions between the peptide and DLC8 and destabilization of the backbone β-strand structure of the peptide. Mutations of the Lys residue to either Ala or Glu lead to somewhat decreased binding affinity between the peptide and DLC8, suggesting that the Lys residue in this position has a relatively small contribution to the binding affinity of the peptide. The mutagenesis study reinforces our earlier conclusion that the interactions between DLC8 and the (K/R)*X*TQT motif-containing peptide are dominated by a combination of side chain and backbone hydrogen-bonding and electrostatic interactions (18).

In summary, we have shown that DLC8 binds to the N-terminal domain of cytoplasmic DIC via a highly conserved (K/R)*X*TQT motif. The data firmly establish that DLC8 is assembled into the cytoplasmic dynein by binding to its intermediate chain located at the base of the motor complex. In addition, we further show that the (K/R)*X*TQT motif represents a general DLC8 recognition sequence in its diverse target proteins. The experimental data presented in this work, together with our earlier structural studies, reinforce the hypothesis that DLC8 probably acts as a multifunctional regulatory protein by binding to a large number of functionally unrelated proteins.

Acknowledgments—We thank Dr. Lap-Chee Tsui for genomic clones of mouse cytoplasmic DIC, Dr. Andreas Strasser for Bim clones used in this study, and Dr. Jim Hackett for careful reading of the manuscript.

REFERENCES

1. Vallee, R. B., and Sheetz, M. P. (1996) *Science* **271,** 1539–1544
2. Hirokawa, N. (1998) *Science* **279,** 519–526
3. King, S. M. (2000) *Biochim. Biophys. Acta* **1496,** 60–75
4. Vaughan, K., and Vallee, R. (1995) *J. Cell Biol.* **131,** 1507–1516
5. Piperno, G., and Luck, D. J. (1979) *J. Biol. Chem.* **254,** 3084–3090
6. Pfister, K. K., Fay, R. B., and Witman, G. B. (1982) *Cell Motil* **2,** 525–547
7. Mitchell, D. R., and Rosenbaum, J. L. (1986) *Cell Motil. Cytoskeleton* **6,** 510–520
8. King, S. M., Barbarese, E., Dillman, J. F., III, Patel-King, R. S., Carson, J. H., and Pfister, K. K. (1996) *J. Biol. Chem.* **271,** 19358–19366
9. Pazour, G. J., Wilkerson, C. G., and Witman, G. B. (1998) *J. Cell Biol.* **141,** 979–992
10. Beckwith, S. M., Roghi, C. H., Liu, B., and Ronald Morris, N. (1998) *J. Cell Biol.* **143,** 1239–1247
11. Jaffrey, S. R., and Snyder, S. H. (1996) *Science* **274,** 774–777
12. Fan, J. S., Zhang, Q., Li, M., Tochio, H., Yamazaki, T., Shimizu, M., and Zhang, M. (1998) *J. Biol. Chem.* **273,** 33472–33481
13. Puthalakath, H., Huang, D. C., O'Reilly, L. A., King, S. M., and Strasser, A. (1999) *Mol. Cell* **3,** 287–296
14. Schnorrer, F., Bohmann, K., and Nusslein-Volhard, C. (2000) *Nat. Cell Biol.* **2,** 185–190
15. Crepieux, P., Kwon, H., Leclerc, N., Spencer, W., Richard, S., Lin, R., and Hiscott, J. (1997) *Mol. Cell. Biol.* **17,** 7375–7385
16. Naisbitt, S., Valtschanoff, J., Allison, D. W., Sala, C., Kim, E., Craig, A. M., Weinberg, R. J., and Sheng, M. (2000) *J. Neurosci.* **20,** 4524–4534
17. Liang, J., Jaffrey, S. R., Guo, W., Snyder, S. H., and Clardy, J. (1999) *Nat. Struct. Biol.* **6,** 735–740
18. Fan, J.-S., Zhang, Q., Tochio, H., Li, M., and Zhang, M. (2000) *J. Mol. Biol.* **306,** 97–108
19. Farmer, B. T., II, Constantine, K. L., Goldfarb, V., Friedrichs, M. S., Wittekind, M., Yanchunas, J., Jr., Robertson, J. G., and Mueller, L. (1996) *Nat. Struct. Biol.* **3,** 995–997
20. Crackower, M. A., Sinasac, D. S., Xia, J., Motoyama, J., Prochazka, M., Rommens, J. M., Scherer, S. W., and Tsui, L. C. (1999) *Genomics* **55,** 257–267
21. Raux, H., Flamand, A., and Blondel, D. (2000) *J. Virol.* **74,** 10212–10216
22. Jacob, Y., Badrane, H., Ceccaldi, P. E., and Tordo, N. (2000) *J. Virol.* **74,** 10217–10222
23. Habura, A., Tikhonenko, I., Chisholm, R. L., and Koonce, M. P. (1999) *J. Biol. Chem.* **274,** 15447–15453
24. Tynan, S. H., Gee, M. A., and Vallee, R. B. (2000) *J. Biol. Chem.* **275,** 32769–32774
25. Benashski, S. E., Harrison, A., Patel-King, R. S., and King, S. M. (1997) *J. Biol. Chem.* **272,** 20929–20935
26. Susalka, S. J., Hancock, W. O., and Pfister, K. K. (2000) *Biochim. Biophys. Acta* **1496,** 76–88
27. Nurminsky, D. I., Nurminskaya, M. V., Benevolenskaya, E. V., Shevelyov, Y. Y., Hartl, D. L., and Gvozdev, V. A. (1998) *Mol. Cell. Biol.* **18,** 6816–6825
28. Mok, Y.-K., Lo, K. W.-H., and Zhang, M. (2001) *J. Biol. Chem.* **276,** 14067–14074